EVALUATION OF INTERFEROMETRIC DIGITAL ELEVATION MODELS DERIVED FROM ERS TANDEM DATA

A. Roth, W. Knöpfle, S. Gebhardt, B. Rabus, D. Scales
DLR, DFD, German Remote Sensing Data Center
D-82230 Oberpfaffenhofen, Germany
Tel: +8153-28-2706, Fax: +8153-28-1445

ISPRS Commission II, Working Group 4

KEY WORDS:

Digital Elevation Model, SAR Interferometry, ERS Tandem

ABSTRACT

The potential of SAR interferometry for the determination of the Earth´s relief is known and is subject to many investigations of the recent years. Most of today's radar satellites enable SAR interferometry, giving new sources for the derivation of digital elevation models (DEM). Common to all is their limitation to repeat pass interferometry. ERS tandem, with 24 hours time difference between both acquisitions, is currently the best available spaceborne repeat pass interferometry configuration in terms of coherence stability and risk of atmospheric distortions. The goal of the ERS tandem DEM quality is to meet the DTED-2 requirements of less than ± 30 m for 90 % of the data. The achievement of this goal was evaluated based on a strip of eight quarter scenes mosaicked to a DEM covering the area of two ERS full scenes. Based on two representative scenes the precision is discussed. It is demonstrated that the DTED requirement can be met for flat and moderately reliefed terrain. Alpine areas, especially forested slopes, require a post processing. The achieved precision will be further enhanced by the Shuttle Radar Topography Mission (SRTM), enabling single pass interferometry.

INTRODUCTION

Since the wording "digital elevation model" was introduced (Miller, 1958) the capabilities of generating, storing and processing DEMs developed dramatically. In the same way the requirements regarding resolution, precision, availability and coverage increased. Today the digital representation of the Earth's relief is precondition to a variety of applications like the consideration of three dimensions in Geographical Information Systems, ground proximity warning systems in aircraft, generation of perspective views and the modeling of geoscientific and atmospheric processes.

Even though the basic principles of SAR interferometry were already described in the mid 70s (Graham, 1974) only since the launch of ERS-1 in 1991 a large amount of suitable data sets became available. Since then, this technique was further developed and became nearly operational. Another improvement could be achieved by operating ERS-1 and ERS-2 in a tandem mode.

DLR's German Remote Sensing Data Center is implementing an operational SAR interferometric processing chain aiming at the derivation of DEMs. The main data sources for this service will be ERS tandem and the Shuttle Radar Topography Mapper SRTM) mission. ERS tandem is currently the best spaceborne SAR repeat pass interferometer while SRTM will be the first single pass interferometry system in space. Especially the latter will allow a global provision of high precision digital elevation information.

INTERFEROMETRIC PRODUCTION CHAIN

In order to support multi-mission capability the overall production chain as well as it's components are following a modular design including standardized interfaces. Depending on mission or project requirements components and modules of the chain can be configured respectively. Figure 1 shows the processing chain and its subsystems.

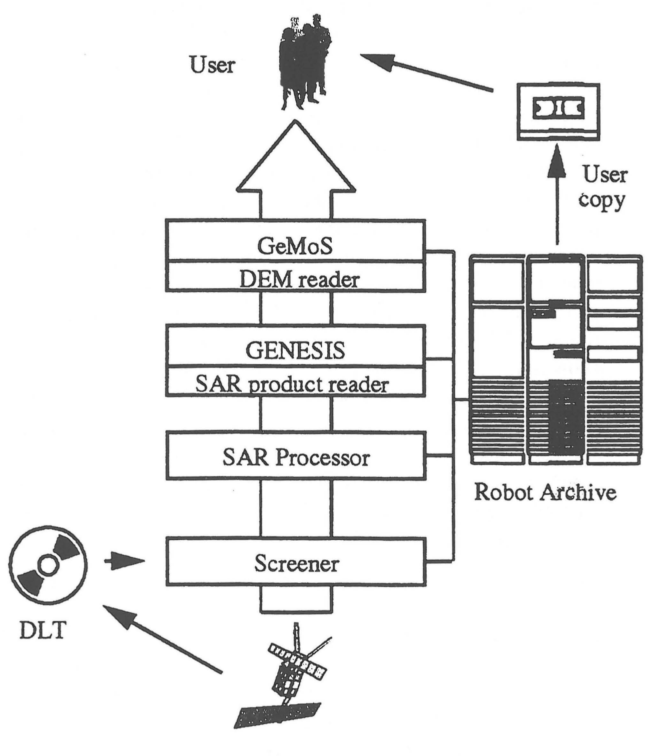

Fig. 1: Interferometric Processing Chain

The entire processing chain comprises four subsystems

- the screening and transcription system
- the SAR processor
- the GENEric System for Interferometric SAR (GENESIS)
- the Geocoding and Mosaicking System (GeMoS)

ERS data can be ingested into the SAR processor, either directly from the recording media (DLT) at the beginning of the chain, or the SAR product reader of GENESIS supports input of standard complex products (e.g. ERS SLC and SLCI).

Starting from complex data of the master and slave images GENESIS processes the coherence map, amplitude images, and the unwrapped phase. This interferometric processing comprises spectral shift filtering, optional slope adaptive filtering, coregistration, multilooking, coherence estimation, flat earth phase removal, and several phase unwrapping procedures (Eineder, 1997). The Minimum Cost Flow algorithm (Costantini, 1996) was found the most suitable unwrapping technique for DEM generation and therefore is applied as standard method.

The Geocoding and Mosaicking System GeMoS finally derives the digital elevation model from the unwrapped phase image. The amplitude and coherence information are required for tiepointing and quality estimation purposes.
Considering the orbit of the master image and the baseline to the slave antenna the absolute phase is converted into height values. This slant range DEM is geocoded into the so called TopoMap product. The product quality is improved by tiepointing and an adjustment. The adjustment requires two different kinds of tiepoints, those used for the correction of the timing parameters and a second applied for phase offset determination. Of coarse, some of these points can be considered for both improvements. In order to cover a large area and to eliminate local distortions due to loss of coherence or atmospheric disturbances individual TopoMaps are assembled to a DEM mosaic. This step comprises statistical outlier tests in order to eliminate gross errors and therewith allows a robust estimation of the resulting heights. By error propagation the quality of the resulting DEM is determined considering the individual quality maps as a priori accuracies (Knöpfle, 1998).
Even though the described processing chain is primarily designed to produce digital elevation models the system outputs intermediate data sets suitable for other applications, like the coherence map, interferograms and amplitude images (Roth, 1998).

EVALUATION

Evaluation Procedure

The accuracy of interferometric DEMs is determined on the basis of individual TopoMaps (DEM of a quarter scene coverage) by comparing pixel by pixel with a reference digital elevation model. Statistics are calculated for the entire image and a color coded difference image, coregistered to the InSAR DEM, is generated for interpretation purposes (Figure 4).
The statistics consider the maximum, minimum, mean values of the differences and their standard deviation, as well as the mean value and the deviation of magnitude and the RMS of the differences. In a table the range of differences is summed into intervals. The goal is that at least 90% of the height values differ by less then ± 30 m to the reference.
For selected test sites the differences were listed against aspect and slope in order to investigate possible dependencies.

The DHM M745, provided by the German military mapping agency AmilGeo, serves as reference. The DHM M745 corresponds to the Digital Terrain Elevation Data set level 2 (DTED-2) standard for West- and DTED-1 for East-Germany. The primary data for the generation of the DHM M745 were obtained by digitizing the topographic map series M745 1:50000. The map sheets were scanned, vectorized, and edited interactively. Then these data were interpolated including optional filtering. Two different software packages were used for this purpose. The DHM M745 shows four different types of artifacts (Roth, 1996):

- Flat areas at local surface extrema (e.g. cut hill tops)
- Edges and line structures at map sheet borders
- Interpolation errors like tiles, stars, strips etc.
- Small cone like features

Some of those artifacts are visible in the DHM M745 subset of the Cologne area (Fig. 2).

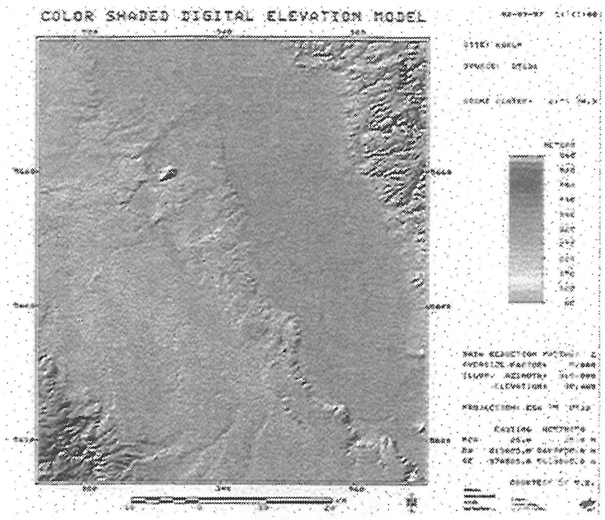

Fig. 2: Reference DEM of Cologne area

Beside the already described artifacts two further effects must be considered when interpreting the differences.
First the DHM M745 represents the Earth's surface without ground coverage. The elevation value is reduced concerning the height of vegetation and buildings. However the radar signal contains the information of the ground coverage as well. It is influenced by several factors like the penetration depths, the surface roughness, it's dielectric properties, and the imaging geometry (incidence angle). E.g. in case of forested areas the interferometric estimated height is a function of the real height of the trees and the penetration depth into the vegetation layer (Floury, 1996).
Secondly, in areas showing rapid elevation changes over time the reference DEM might be out of date. Comparing the DEM of Figure 2, the interferometric DEM in Figure 3, and the corresponding difference image in Figure 4 highlights such an effect. The reference DEM doesn't contain the surface mining areas at all causing those areas to appear even outside the color coded range of ±100 m. Additionally, the mapped rubble and coal stocks changed over this time intervall as well.

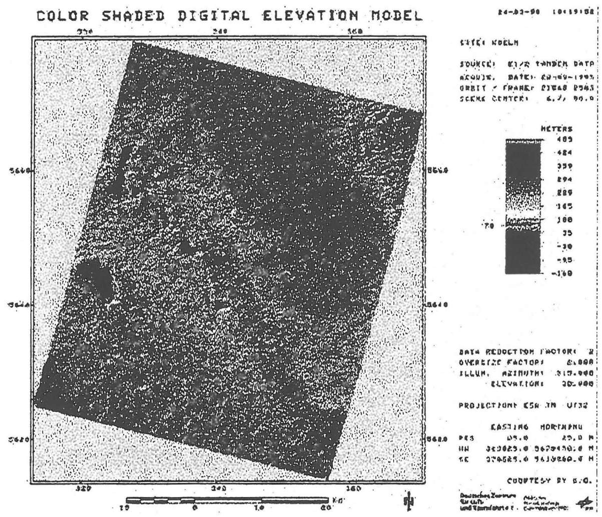

Figure 3: Interferometric DEM of the Cologne area

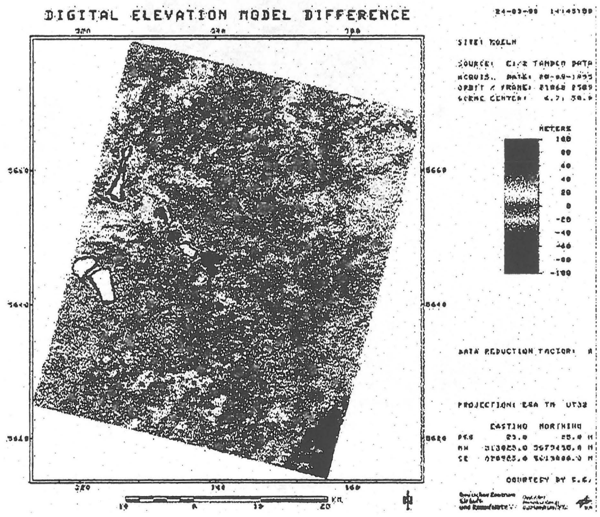

Figure 4: Difference Image of Cologne area

Test Sites

A 200 km x 100 km area of Bavaria ranging from the northern edge of the Alps to Nürnberg was selected as test region. It corresponds to the coverage of eight ERS SLC quarter scenes. The area shows different types of terrain – a mountainous part in the south, the flat rubble plains around Munich and Augsburg, and the hilly regions of the Hallertau and Fränkische Alb. The interferometric DEM is shown in Figure 5.

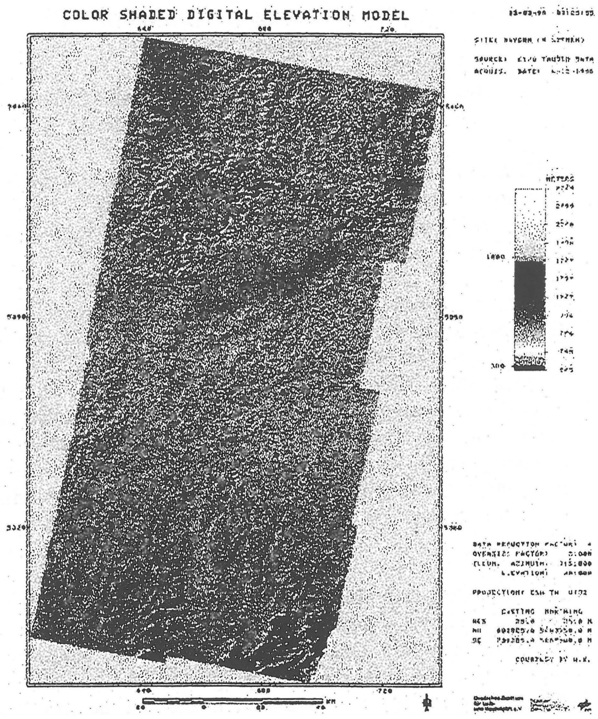

Figure 5: Interferometric DEM of Bavarian test site

The strip was processed from the ERS-1/ERS-2 tandem orbits 22970/3297, acquired on December 6th and 7th, 1995. The eight quarter scenes of the frames 2619 and 2637 were considered, showing effective baselines of 90 to 95 m.
The quality of the ERS tandem InSAR digital elevation model will be described based on two representative TopoMaps, covering mountainous, hilly, and flat terrain. The test sites are named by the cities Weilheim and Munich located within the respective data set.

RESULTS

Weilheim Test Site – Slope Dependency

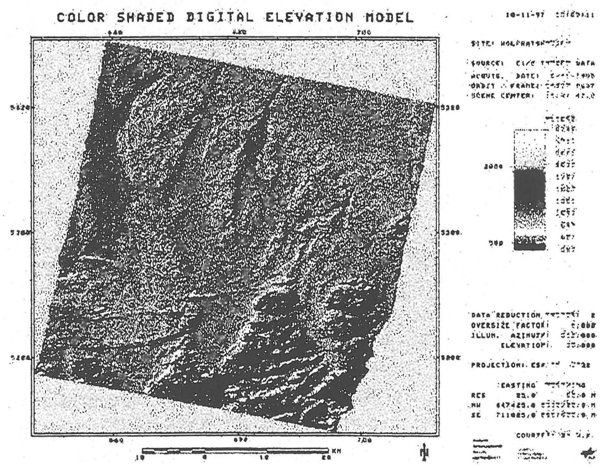

Figure 6: InSAR DEM of Weilheim area

Approximately 2/3 of the Weilheim test area (frame 2637, quarter 1) is moderately reliefed. However, the other third is covered by parts of the northern mountain ridges of the Alps (Figure 6). The elevation within the TopoMap ranges from 500 m to 2800 m. The maximum slope is 74.0°, the minimum 0.0°. The mean slope was determined as 6.4° with a standard deviation of 9.6°.

The results of the calculations (reference DEM minus InSAR DEM) are displayed as difference image in Figure 7 and the corresponding statistics in Table 1 and Table 2.

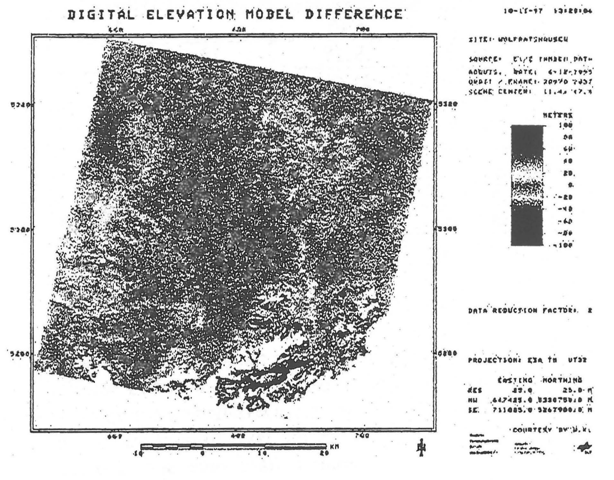

Figure 7: Difference Image of Weilheim area

Maximum value of differences	865.00 m
Minimum value of differences	-1475.00 m
Mean value of differences	-9.88 m
Std. deviation of differences	116.49 m
Mean value of magnitude	36.72 m
Std. deviation of magnitude	111.46 m
RMS of differences	117.35 m

Table 1: Statistics of difference values

Range of differences	percentage	+	
0 m	5.07	-	-
1 m	16.03	11.19	4.84
2 m	25.86	16.48	9.38
3-4 m	42.95	25.75	17.21
5-8 m	68.47	39.40	29.07
9-16 m	82.77	48.40	34.36
17-32 m	86.77	50.52	36.25
33-64 m	89.10	51.70	37.40
65-128 m	92.78	53.68	39.10
>128 m	100.00	56.80	43.20

Table 2: Percentage of difference classes

The statistics of Tables 1 and 2, as well as Figure 7 show that the predominant part of image coincides with the reference model. The color range from yellow to light blue indicates differences of ± 20 m. A comparison of the difference image with an composition of the amplitude and coherence images demonstrates the correspondence of forests with areas where the interferometric DEM is higher than the reference model.

The minimum and maximum values appear at the edge of the image where it intersects a lake. Water totally decorrelates introducing a noise pattern on the surface. A special filter was implemented to eliminate this effect. However, the current version of the software doesn't completely eliminate corrupted pixels at the edge of the image.

Large differences appear in the mountainous part, due to the steep slopes covered with forests. Forests, as typical volume scatterers, are sensitive to structure variations between the two acquisitions caused by wind effects or vegetation growth. Both lead to a loss of coherence. The fringe frequency increases with steeper slopes. However, the fringe information is corrupted by noise induced by the loss of coherence. In this case, fringes are simply lost, leading to a systematic underestimation of the terrain height. This error is even enhanced by layover and shadow.

In order to investigate the dependency of the differences on slope and aspect the magnitude of differences were listed against slope classes for slopes facing towards (Table 4) and away from the sensor (Table 5). Table 3 contains the statistics of all slopes, regardless the slope's orientation.

differ-ences	0° slope	1°-6° slope	7°-12° slope	13°-18° slope	>18° slope
0-4 m	19.98 %	19.07 %	2.91 %	0.63 %	0.38 %
5-9 m	13.08 %	12.39 %	2.46 %	0.65 %	0.42 %
10-19 m	3.43 %	5.10 %	2.09 %	0.91 %	0.77 %
20-29 m	0.17 %	0.43 %	0.48 %	0.46 %	0.62 %
30-39 m	0.05 %	0.10 %	0.17 %	0.25 %	0.49 %
40-49 m	0.03 %	0.04 %	0.10 %	0.17 %	0.40 %
>49 m	0.67 %	1.10 %	1.47 %	2.08 %	6.45 %
Σ	37.41 %	38.23 %	9.68 %	5.15 %	9.53 %

Table 3: Slopes of all aspects

The scene was separated into four aspects. 17% of the image pixels are oriented towards as well as away from the satellite, while 12% are looking against and 17% in the azimuth direction. 37% are not sloped. The percentages of the following tables consider the corresponding aspect as 100%.

differ-ences	1°-6° slope	7°-12° slope	13°-18° slope	>18° slope	Σ
0-4 m	33.6 %	4.9 %	1.0 %	0.5 %	40.0 %
5-9 m	21.3 %	3.8 %	1.0 %	0.6 %	26.7 %
10-19 m	7.7 %	2.7 %	1.2 %	1.0 %	12.6 %
20-29 m	0.7 %	0.4 %	0.5 %	0.7 %	2.3 %
30-39 m	0.2 %	0.3 %	0.3 %	0.7 %	1.5 %
40-49 m	0.1 %	0.2 %	0.3 %	0.6 %	1.2 %
>49 m	2.0 %	2.2 %	2.9 %	8.6 %	15.7 %
Σ	65.6 %	14.5 %	7.2 %	12.7 %	100.0 %

Table 4: Aspect "towards the sensor"

differ-ences	1°-6° slope	7°-12° slope	13°-18° slope	>18° slope	Σ
0-4 m	31.7 %	5.4 %	1.1 %	0.6 %	38.8 %
5-9 m	19.6 %	4.3 %	1.1 %	0.7 %	25.7 %
10-19 m	8.3 %	3.6 %	1.4 %	1.2 %	14.5 %
20-29 m	0.7 %	0.9 %	0.8 %	0.9 %	3.3 %
30-39 m	0.1 %	0.3 %	0.4 %	0.7 %	1.5 %
40-49 m	0.1 %	0.1 %	0.2 %	0.5 %	0.9 %
>49 m	1.4 %	2.2 %	3.0 %	8.7 %	15.3 %
Σ	61.9 %	16.8 %	8.0 %	13.3 %	100.0 %

Table 5: Aspect "away from the sensor"

The tables show the known effect that increasing slopes lead to larger height errors. However, dependencies between slope and aspect and height errors could not be determined. The better resolution of SAR data on backside slopes causes a lower fringe frequency in the slant range domain. It was expected that this could lead to a better height accuracy, especially when those slopes show less coherence due to vegetation. However in this case the decorrelation of the forested slopes corrupted the fringes on all slopes in the same way.

Munich Test Site – Local Distortions and Tiepoints

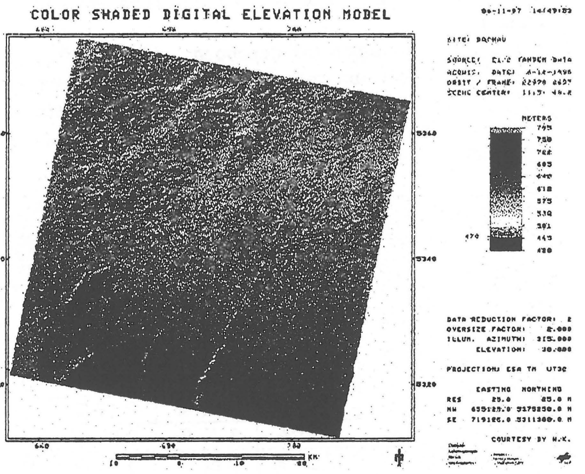

Figure 8: InSAR DEM of Munich area

Approximately 2/3 of the Munich test area (frame 2637, quarter 4) is a slightly tilted rubble plain formed during the last glacial period (Figure 8). The remaining third is moderately reliefed. The elevation within the TopoMap ranges from 470 m to 780 m. The maximum slope is 33.0°, the minimum 0.0°. The mean slope was determined as 1.9°, with a standard deviation of 2.7°. The results of the calculations (reference DEM minus InSAR DEM) are displayed as difference image in Figure 8 and the corresponding statistics in Table 6 and Table 7.

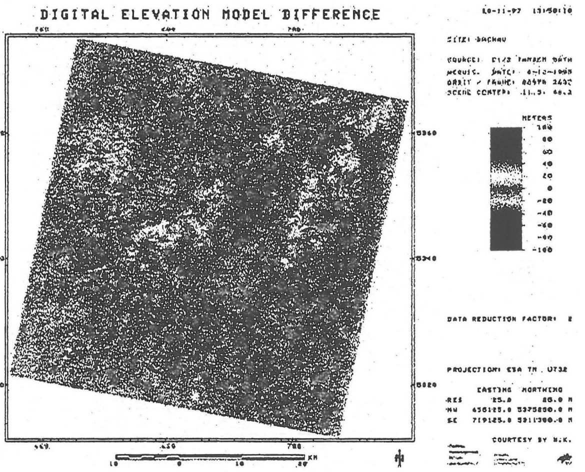

Figure 9: Difference Image of Munich area

The following results were derived:

Maximum value of differences	105.00 m
Minimum value of differences	-148.00 m
Mean value of differences	-1.49 m
Std. deviation of differences	6.68 m
Mean value of magnitude	5.20 m
Std. deviation of magnitude	4.45 m
RMS of differences	6.84 m

Table 6: Statistics of difference values

Range of differences	percentage	+	
0 m	6.46	-	-
1 m	19.18	12.56	6.63
2 m	31.42	18.15	13.27
3-4 m	53.11	27.22	25.88
5-8 m	81.56	37.56	44.00
9-16 m	97.69	42.59	55.11
17-32 m	99.90	43.32	56.57
33-64 m	99.99	43.35	56.64
>64 m	100.00	43.36	56.64

Table 7: Percentage of difference classes

The difference image, as well as the statistics of Tables 6 and 7, demonstrate the high correspondence between interferometric and reference elevation model. Deviations exist again where the border of the image covers the lake Ammersee (south-western edge). In the image center a dark blue spot indicates much higher elevation (60-80m) within the interferometric DEM. Here, a dump is mapped that is not considered by the reference data set (Figure 10).

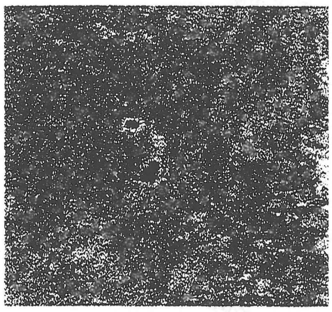

Figure 10: Subset of Difference Image – Dump

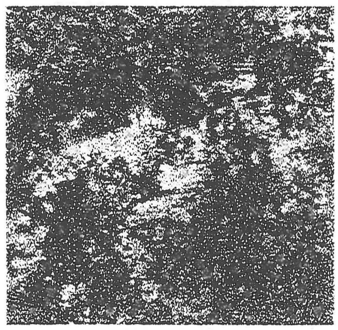

Figure 11: Subset of Difference Image – Agricultural Fields

Areas in light green and yellow differ about 10-20 m from the reference. Here the interferometric DEM is systematically lower than the reference. It mainly coincides with agricultural fields, grass- and wetland (Figure 11). This effect neither correlates with the terrain, nor does it show the typical appearance of atmospheric artifacts. It is local and in particular the areas of the highest deviations (up to 20m) reflect exactly the field structures. The coherence of these areas is slightly lower compared to the surrounding. This indicates changes of the surface or it's reflection behavior causing slight phase shifts and thereby a higher elevation.

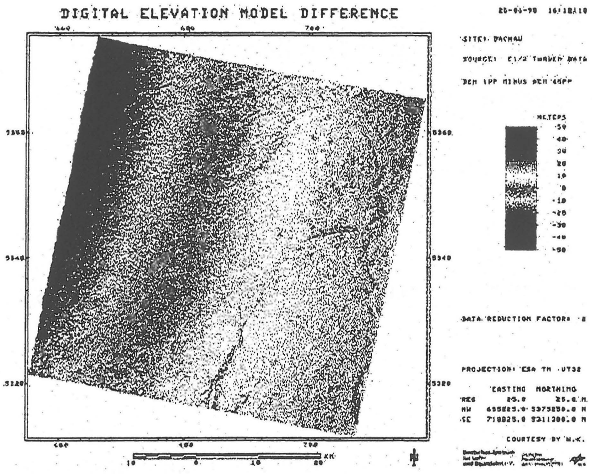

Figure 12: Difference Image of interferometric DEMs

As already described, the processing comprises an adjustment based on tiepoints. The presented accuracy could be achieved by the consideration of a significant number of tiepoints. In this case 17 timing, 30 phase, and 16 tiepoints, suitable for the improvement of the timing and phase parameters were measured. Figure 12 shows the difference image between interferometric DEMs produced considering 45 against only one phase tiepoint. In both cases the timing parameters in azimuth and range were corrected.

One phase tiepoint allows only the determination of an offset. Mainly due to baseline uncertainties the entire image is tilted. Also, possible phase unwrapping errors can introduce phase ramps. Without an adjustment of the phase values the DEM is tilted across range leading to ± 30 m discrepancies at the western and eastern edges.

CONCLUSION

The test data of this evaluation show extremely good quality. Most parts are highly coherent. Local and atmospheric distortions are low and do not reduce the precision significantly. Therefore, the goal of a precision better than ± 30 m for 90% of the InSAR DEM data could be achieved with only one ERS tandem data set. The alpine part of the Weilheim test area, however, requires post processing in order to mask and eliminate erroneous pixels. The other types of terrain – flat plain and moderately reliefed areas –fulfill the requirement directly. Data sets not fulfilling this preconditions need the consideration of several tandem pairs and mosaicking.

A dependency of height precision on the slope's aspect could not be shown. Low coherence, due to the coverage of the corresponding slopes with forests, caused loss of fringes and thereby a systematic underestimation of the mountain height, regardless of the slope's aspect.

The consideration of at least 10 location and 30 phase tiepoints for every scene is required, in order to achieve the presented accuracy.

Even though the ERS repeat pass interferometry is hampered by several factors like baseline uncertainties, decorrelation, atmospheric distortions etc., high quality DEMs can be generated.

REFERENCES

Costantini, M., 1996. A phase unwrapping method based on network programming. Proceedings of FRINGE 96 ESA Workshop on Applications of ERS SAR Interferometry, Zürich, Vol. I, pp. 261-272

Eineder, M., Adam, N., 1997. A Flexible System for the Generation of Interferometric SAR Products, Proceedings of IGARSS'97

Floury, N., et al, 1996. Interferometry for Forest Studies. Proceedings of FRINGE 96 ESA Workshop on Applications of ERS SAR Interferometry, Zürich, Vol. II, pp. 57-70

Graham, L.C., 1974. Synthetic interferometer radar for topographic mapping, Proceedings of the IEEE, 62(6), pp. 763-768

Knöpfle W., Strunz G., Roth A., 1998. Mosaicking of Digital Elevation Models derived by SAR Interferometry, Paper submitted to ISPRS Com. IV Symposium, Stuttgart, Sep. 7-10 1998

Miller, C.L., Laflamme, R.A., 1958. The Digital Terrain Model – Theory and Application, Photogrammetric Engineering, 24, pp.433-442

Roth, A., Strunz, G., Knöpfle, W., 1996. Transformation und Qualitätsanalyse des Digitalen Höhenmodells DHM M745 für die E-Plus Mobilfunk GmbH, Internal Report

Roth, A., Knöpfle, W., Hubig, M., Adam, N., 1998. Operational Interferometric SAR Products, Proceedings of IGARSS 98